NASA TN D-451

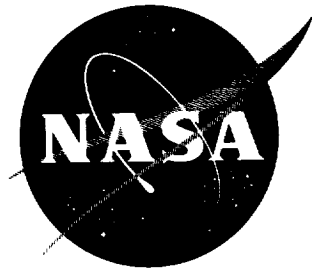

p. 20

TECHNICAL NOTE
D-451

FLUTTER RESEARCH ON SKIN PANELS

By Eldon E. Kordes, Weimer J. Tuovila, and Lawrence D. Guy

Langley Research Center
Langley Field, Va.

NATIONAL AERONAUTICS AND SPACE ADMINISTRATION
WASHINGTON
September 1960

NATIONAL AERONAUTICS AND SPACE ADMINISTRATION

TECHNICAL NOTE D-451

FLUTTER RESEARCH ON SKIN PANELS

By Eldon E. Kordes, Weimer J. Tuovila, and Lawrence D. Guy

SUMMARY

Representative experimental results are presented to show the current status of the panel flutter problem. Results are presented for unstiffened rectangular panels and for rectangular panels stiffened by corrugated backing. Flutter boundaries are established for all types of panels when considered on the basis of equivalent isotropic plates. The effects of Mach number, differential pressure, and aerodynamic heating on panel flutter are discussed. A flutter analysis of orthotropic panels is presented in the appendix.

INTRODUCTION

The problem of panel flutter has become critical with the inception of hypersonic and reentry vehicles, particularly when the exposed skin panels are not designed to carry appreciable structural loads. For this type of exposed surfaces, panel flutter becomes the primary weight-establishing design criterion. Some typical skin panels for hypersonic and reentry vehicles are shown in figure 1.

The panel at the upper left of figure 1 is a simple unstiffened flat plate. For a multibay region of the exposed surface which is made up of sheet and stringers, as shown at the upper right of figure 1, the portion of the sheet between stringers is considered to act as an independent panel. For the purpose of this paper these two panel types are referred to as unstiffened panels. The two panel types shown at the bottom of figure 1 are stiffened by corrugations. The corrugation pitch is small and the panel and corrugated backing act as a unit. Both of the corrugation-stiffened panels have a much higher stiffness parallel to the corrugation than in the other direction.

The flutter behavior of these types of panels has been the subject of many theoretical investigations. Comparison of the predictions of theory with experimental flutter data shows marked disagreement for all but the simplest configurations. Therefore, experimentally determined

flutter boundaries must be relied on for design information. Such experimental work is presently in progress and some recent flutter results for rectangular panels are presented in this paper.

SYMBOLS

$A = R_x - 2n^2\pi^2\left(\frac{l}{w}\right)^2 \frac{D_{xy}}{D_x}$

$\overline{A} = \overline{R}_x - 2n^2\left(\frac{l}{w}\right)^2_{EFF}$

A_o enclosed area of torque cell

$B = k^2 + n^2\pi^2\left(\frac{l}{w}\right)^2 R_y - n^4\pi^4\left(\frac{l}{w}\right)^4 \frac{D_y}{D_x}$

$\overline{B} = \bar{k}^2 + n^2\left(\frac{l}{w}\right)^2_{EFF} \overline{R}_y - n^4\left(\frac{l}{w}\right)^4_{EFF} \frac{D_x D_y}{D_{xy}^2}$

D_{EFF} flexural rigidity of equivalent isotropic plate

D_x flexural rigidity of orthotropic plate in x-direction

D_y flexural rigidity of orthotropic plate in y-direction

D_{xy} twisting stiffness of orthotropic plate relative to x- and y-directions

E Young's modulus of elasticity

G shear modulus of elasticity

h normalized depth of corrugations

k frequency parameter, $\omega l^2\sqrt{\frac{\gamma}{D_x}}$

$\bar{k} = \frac{k}{\pi^2}$

L lateral aerodynamic loading

l, w dimensions of orthotropic plate (see sketch 1 in appendix)

l_{EFF}, w_{EFF} dimensions of equivalent isotropic plate

M	Mach number
N_x, N_y	midplane stresses in x- and y-directions
n	integer
Δp	differential static pressure
q	dynamic pressure, $\rho U^2/2$

$R_x = N_x l^2/D_x$

$\bar{R}_x = R_x/\pi^2$

$R_y = N_y l^2/D_x$

$\bar{R}_y = \frac{R_y}{\pi^2}\frac{D_x}{D_{xy}}$

Re	real part
T_o	stagnation temperature
t	thickness of material
t_{EFF}	thickness of equivalent isotropic plate
U	velocity of air flow
W	lateral deflection of panel
$\bar{W}_n$	deflection function (eq. (3))
x,y,z	Cartesian coordinates (see sketch 1)

$x_1 = \frac{x}{l}$

$\beta = \sqrt{M^2 - 1}$

γ	mass of plate per unit area
λ	dynamic-pressure parameter, $2ql^3/\beta D_x$

λ_{cr}	critical value of λ
ν	Poisson's ratio
ρ	mass density of air
τ	time
ω	circular frequency

FLUTTER OF UNSTIFFENED PANELS

Effect of Panel Aspect Ratio

Experimental results for the flutter of unstiffened rectangular flat panels are shown in figure 2. In this figure the abscissa is the panel length-width ratio on a log scale and the ordinate is a modified-thickness-ratio parameter which has been shown by theory to be the primary panel-flutter parameter. In this thickness-ratio parameter, t/l is the ratio of panel thickness to panel length, M is the Mach number, q is the dynamic pressure at flutter, and E is the Young's modulus of the material. In figure 2 a vertical bar represents the test results for panels with a given length-width ratio but with varying sizes, materials, Mach number, and temperature. The number by each bar is the number of test points and the length of the bar indicates the scatter of the results. An envelope curve has been drawn to enclose the upper end of the scatter band and hence should be a conservative boundary. The flutter region lies below this curve. Note that many of the panels tested were very long and narrow; such panels are of considerable practical importance and flutter data on them have not been available until recently. Because flutter amplitudes are usually limited by the nonlinear behavior of the panels, panel flutter is considered to be primarily a fatigue problem. The severity of the flutter is therefore of interest. In the tests represented by the results in figure 2, panels with lower length-width ratios usually exhibited relatively large amplitude vibrations and many panels failed before flutter could be stopped. On the other hand, the long, narrow panels exhibited mild flutter. In some cases these flutter vibrations were difficult to distinguish from the background noise without a spectral analysis.

The thickness-ratio parameter used in figure 2 does not contain all the factors that are known to affect the flutter boundaries - hence, the scatter. However, this flutter parameter has proven to be very useful in comparing the results from a wide variety of test conditions.

Effect of Differential Pressure

One of the factors not accounted for in the parameter is the effect of differential pressure. Previous investigators (see, for example, refs. 1 and 2) have shown that small amounts of differential pressure, either positive or negative, reduce the thickness required to prevent flutter. The results presented in figure 2 were obtained by holding the differential pressure as near to zero as possible. This was done for two reasons. First, the design information obtained should be conservative, and second, the influence of other factors can be studied without being masked by scatter caused by varying differential pressures.

Effect of Midplane Stresses

Another important effect on panel flutter is the influence of stresses and buckling caused in the panel by aerodynamic heating and loading. This effect has been recently investigated in detail by means of a series of tests like the one illustrated in figure 3. This figure shows the history of a typical tunnel run at $M = 3$, a stagnation temperature of 500° F, a dynamic pressure of 3,100 psf, and zero differential pressure. During this run the panel temperature varied with time as shown. All other test conditions were held constant. The panel did not flutter until the temperature reached 150°, where flutter started as indicated by the open symbol. When the panel temperature reached 300° the flutter stopped, as indicated by the solid symbol. Theory predicts that as a panel is heated the effects of thermal expansion will develop compressive midplane stresses that increase the susceptibility to flutter. After buckling, the additional temperature rise increases the depth of buckles, thereby stiffening the panel and finally stopping the flutter.

The results of many such runs are shown in figure 4. The thickness-ratio parameter for flutter is shown as a function of the panel temperature rise. These results were obtained on aluminum panels with a length-width ratio of 10 tested at a Mach number of 3. Only panel thickness, stagnation temperature, and dynamic pressure were changed from test to test. Again the open symbols indicate flutter starts and the solid symbols indicate flutter stops. If these results are compared with the results shown in figure 2 it can be seen that the maximum value of the thickness-ratio parameter for the start of flutter from figure 4 agrees with the envelope curve in figure 2 for an l/w of 10. Furthermore, the range of scatter of data below the envelope agrees with the range obtained by varying the temperature only. Thus, these results indicate that midplane stress is the primary cause of scatter.

Effect of Mach Number

The effect of Mach number on panel flutter is shown in figure 5, where the thickness-ratio parameter is plotted against Mach number at flutter. The tests were run at zero differential pressure on initially flat panels buckled by heat. The vertical bars represent the range of the test results for each Mach number and the number by each bar represents the number of test points. Any substantial Mach number trend in these data is obscured by the scatter. Again a large part of this scatter is probably due to differences in midplane stress.

FLUTTER OF CORRUGATION-STIFFENED PANELS

Next, consider the flutter of the panels stiffened by corrugations shown in figure 1. Tests have been run on both types of corrugation-stiffened panels shown. The panels were tested both with the flow direction along the corrugations and with the flow across the corrugations. The flutter results for the corrugation-stiffened panels with the flow direction across the corrugations are presented in figure 6. In this figure, the thickness-ratio parameter on the ordinate is based on an effective thickness, and the length-width ratio on the abscissa is based on an effective width. The length l is taken to be the actual length. The effective thickness and width are the dimensions of an equivalent isotropic plate that would have the same important stiffness characteristics as the actual orthotropic, corrugation-stiffened panel. (See the appendix.) The equivalent isotropic plate is found to have a greatly reduced structural width. Hence, almost-square corrugation-stiffened panels have large effective length-width ratios. It should be pointed out that this effective length-width ratio is a structural ratio and that the aerodynamic length-width ratio of the original panel is unchanged.

Using these effective dimensions allows the results for the various types of panels to be compared on the same basis. In figure 6 the solid bars are the flutter results for the corrugation-stiffened panels and the shaded bars are the results for unstiffened panels from figure 2. The envelope curve from figure 2 has been extended to include the present data. This envelope has been drawn as a continuous curve even though the results are for entirely different types of panels. At present there is no experimental verification that the flutter results for corrugation-stiffened panels with effective length-width ratio less than 10 will agree with the results for unstiffened panels. The small variation of the thickness-ratio parameter over a wide range of the length-width ratio indicates that stiffening the panel across the width has very little beneficial effect in preventing flutter. Incidentally, some of the corrugation-stiffened panels tested represented an actual design for a hypersonic vehicle. These panels fluttered at unsatisfactorily low

dynamic pressures. A "fix" was obtained on these panels by welding small strips to the back of the corrugations, and flutter was thereby prevented for dynamic pressures of twice the original flutter value.

Results for stiffened panels with the flow direction along the corrugations do not appear in this figure because no flutter was obtained up to the maximum tunnel conditions, which were about 40 percent greater than the conditions required for flutter of the best corrugation-stiffened panel shown. The panels with corrugations alined with the flow are very stiff along the length, and on an equivalent basis the value of the thickness-ratio parameter would be very large - well outside the flutter region.

For all the corrugation-stiffened panels that fluttered, the flutter was very sudden and very severe. The panels failed unless flutter was stopped in a few seconds.

PANEL FLUTTER ON X-15 AIRPLANE

The material presented so far summarizes the present understanding of the flutter of flat panels based on theoretical calculations and experimental results. It is of interest to examine these results in terms of a full-scale vehicle. The X-15 was designed as a manned hypersonic and reentry vehicle and the exposed surfaces of this vehicle consist of several of the panel types shown in figure 1. Figure 7 shows the X-15 and some of the regions where unstiffened panels and corrugation-stiffened panels are used. The shaded areas represent fairing panels stiffened by corrugations across the flow direction and the black areas represent unstiffened panels that have a length-width ratio of 10. Wind-tunnel tests on the full-scale vertical tail and on full-scale panels from the side fairings have shown that panel flutter exists in the operating range of the X-15. Severe vibrations that appeared during the early flights were in part traced to flutter of these side-fairing panels.

The flutter data for panels from the X-15 are shown in figure 8 in relation to the flutter boundary established in figure 6. The ordinate is the familiar thickness-ratio parameter based on the panel length and effective thickness and the abscissa is the ratio of the panel length to the effective width. The circle point represents a flutter point for the unstiffened panel on the vertical tail. This was not a boundary point (as indicated by the arrow); it was obtained from wind-tunnel tests for conditions beyond the design range of the vehicle. The square symbol at l/w_{EFF} of 150 was a flutter-boundary point obtained in flight on one of the corrugation-stiffened panels from the side fairing, and the square symbols at l/w_{EFF} of 4 represent flutter-boundary points from

wind-tunnel tests of another fairing panel obtained at two different Mach numbers. These results are gratifying. The results for the panel with $l/w_{EFF} = 4$ are seen to agree with the envelope curve established in figure 2 by the results for unstiffened panels. This agreement indicates that the flutter of corrugation-stiffened and unstiffened panels can be satisfactorily compared on the basis of equivalent isotropic plates. For the panel at $l/w_{EFF} = 4$, a single strap riveted to the back of this panel doubled the dynamic pressure required for flutter; three straps were necessary to prevent flutter within the design range of the vehicle.

CONCLUDING REMARKS

Experimental flutter results have been presented for panel configurations including long narrow panels and corrugation-stiffened panels for which previously no information was available. Aerodynamic heating was shown to have considerable effect on the flutter results. Flutter boundaries were established for all types of panels when considered on the basis of equivalent isotropic plates. The results of wind-tunnel tests were shown to agree well with flight data obtained from a hypersonic vehicle. Also, the fact has been established that from the standpoint of flutter, corrugation-stiffened panels should be designed so that the flow is along the corrugations in order to obtain the greatest flutter margin.

Langley Research Center,
National Aeronautics and Space Administration,
Langley Field, Va., April 12, 1960.

APPENDIX

FLUTTER ANALYSIS OF ORTHOTROPIC PLATES

The panel configuration to be analyzed herein consists of a simply supported flat plate mounted in a rigid wall with supersonic air flowing over the top surface. The plate has different elastic properties in the flow direction than in the direction across the flow. The plate has a length l in the flow direction and a width w and is subjected to constant midplane forces of intensities N_x and N_y (positive in compression).

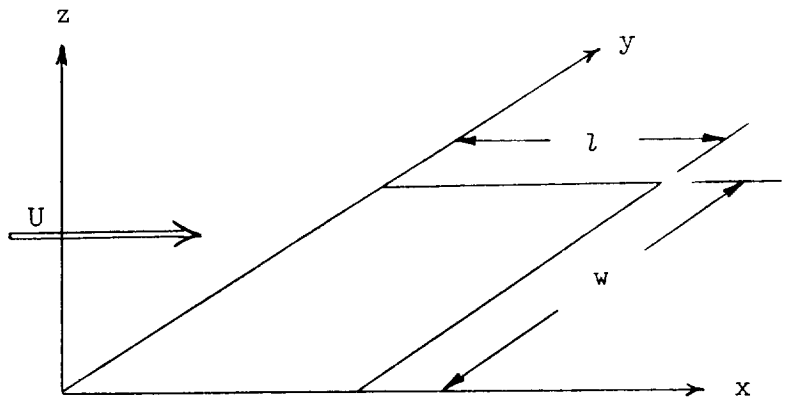

Sketch 1

In the analysis, small-deflection thin-plate theory for anisotropic plates (see ref. 3) is assumed to apply. The equilibrium equation and boundary conditions are:

$$\left.\begin{aligned} &D_x \frac{\partial^4 W}{\partial x^4} + 2D_{xy} \frac{\partial^4 W}{\partial x^2 \partial y^2} + D_y \frac{\partial^4 W}{\partial y^4} + N_x \frac{\partial^2 W}{\partial x^2} + N_y \frac{\partial^2 W}{\partial y^2} + \gamma \frac{\partial^2 W}{\partial \tau^2} = L(x,y,\tau) \\ &W(0,y,\tau) = W(l,y,\tau) = W(x,0,\tau) = W(x,w,\tau) = 0 \\ &\frac{\partial^2 W}{\partial x^2}(0,y,\tau) = \frac{\partial^2 W}{\partial x^2}(l,y,\tau) = \frac{\partial^2 W}{\partial y^2}(x,0,\tau) = \frac{\partial^2 W}{\partial y^2}(x,w,\tau) = 0 \end{aligned}\right\} \quad (1)$$

where $W(x,y,\tau)$ is the lateral deflection of the plate and $L(x,y,\tau)$ is the lateral load per unit area due to aerodynamic pressure. The flexural rigidities of the plate in the x- and y-directions are D_x

and D_y, respectively, D_{xy} is the twisting stiffness relative to the x- and y-directions, and γ is the mass of the plate per unit area.

It is assumed that the air forces yielded by linearized static aerodynamic theory give an adequate approximation. The flutter analysis that follows is based on aerodynamic strip theory and follows the procedure given in reference 4 for the flutter of isotropic plates.

The aerodynamic loading is given by the simple Ackeret value and equation (1) becomes

$$D_x \frac{\partial^4 W}{\partial x^4} + 2D_{xy} \frac{\partial^2 W}{\partial x^2 \partial y^2} + D_y \frac{\partial^4 W}{\partial y^4} + N_x \frac{\partial^2 W}{\partial x^2} + N_y \frac{\partial^2 W}{\partial y^2} + \gamma \frac{\partial^2 W}{\partial \tau^2} + \frac{2q}{\beta} \frac{\partial W}{\partial x} = 0 \quad (2)$$

where q is the dynamic pressure $\rho U^2/2$, $\beta = \sqrt{M^2 - 1}$, and M is the Mach number.

For harmonic motion of the simply supported plate the lateral deflection can be written in the form

$$W = \mathrm{Re}\left[\bar{W}_n(x) \sin \frac{n\pi y}{w} e^{i\omega\tau}\right] \quad (3)$$

where ω is the circular frequency.

Substituting equation (3) into equation (2) yields

$$\bar{W}_n{}^{IV} - 2n^2\pi^2\left(\frac{l}{w}\right)^2 \frac{D_{xy}}{D_x} \bar{W}_n'' + n^4\pi^4\left(\frac{l}{w}\right)^4 \frac{D_y}{D_x} \bar{W}_n + R_x \bar{W}_n''$$

$$- n^2\pi^2 R_y \left(\frac{l}{w}\right)^2 \bar{W}_n + \lambda \bar{W}_n' - k^2 \bar{W}_n = 0 \quad (4)$$

and the associated boundary conditions

$$\bar{W}_n(0) = \bar{W}_n''(0) = \bar{W}_n(1) = \bar{W}_n''(1) = 0$$

where the primes denote differentiation with respect to $x_1 = \frac{x}{l}$ and

$$\left.\begin{aligned} R_x &= \frac{N_x l^2}{D_x} & \lambda &= \frac{2ql^3}{\beta D_x} \\ R_y &= \frac{N_y l^2}{D_x} & k^2 &= \frac{\gamma l^4}{D_x}\omega^2 \end{aligned}\right\} \quad (5)$$

Equation (4) can be rewritten:

$$\bar{W}_n^{IV} + A\bar{W}_n'' + \lambda\bar{W}_n' - B\bar{W}_n = 0 \tag{6}$$

where

$$\left.\begin{aligned} A &= R_x - 2n^2\pi^2\left(\frac{l}{w}\right)^2 \frac{D_{xy}}{D_x} \\ B &= k^2 + n^2\pi^2\left(\frac{l}{w}\right)^2 R_y - n^4\pi^4\left(\frac{l}{w}\right)^4 \frac{D_y}{D_x} \end{aligned}\right\} \tag{7}$$

Equations (6) and (7) are now in the same form as equations (7) and (8), respectively, of reference 4, and the solutions presented therein in terms of the parameters A, B, and λ apply to the present problem. The results presented in reference 4 show that the value of λ_{cr} is essentially dependent on the parameter A and that the results for a plate aspect ratio of 1 could be extended to apply to other aspect ratios through the use of this parameter. It was shown also that coupling between the various modes in the y-direction is slight and that λ_{cr} is virtually independent of the value of R_y.

Examination of the parameters of the present problem in equations (5) and (7) shows that the orthotropic plate properties can be replaced by the properties of an equivalent isotropic plate that has the same important stiffness characteristics for flutter. From aerodynamic consideration the equivalent plate must have the same length l and plate stiffness D_x in the flow direction as the orthotropic plate. Since the value of λ_{cr} is essentially dependent on A, the effective structural aspect ratio for the equivalent isotropic plate can be determined from the last term in A by means of the relation

$$\left(\frac{l}{w}\right)_{EFF} = \frac{l}{w}\sqrt{\frac{D_{xy}}{D_x}} \tag{8}$$

where $\left(\frac{l}{w}\right)_{EFF}$ is the effective length-width ratio of the equivalent plate.

Equation (7) can be rewritten:

$$\left.\begin{aligned} \bar{A} &= \bar{R}_x - 2n^2\left(\frac{l}{w}\right)^2_{EFF} \\ \bar{B} &= \bar{k}^2 + n^2\left(\frac{l}{w}\right)^2_{EFF}\bar{R}_y - n^4\left(\frac{l}{w}\right)^4_{EFF}\frac{D_x D_y}{D_{xy}^2} \end{aligned}\right\} \tag{9}$$

where

$$\bar{R}_x = \frac{R_x}{\pi^2}$$

$$\bar{R}_y = \frac{R_y}{\pi^2}\frac{D_x}{D_{xy}}$$

$$\bar{k} = \frac{k}{\pi^2}$$

Since λ_{cr} has been shown to be essentially independent of $\bar{R}_y$, the essential properties of the equivalent isotropic plate are defined by the three quantities l_{EFF}, D_x, and w_{EFF}. The last term in $\bar{B}$ appears as a constant and hence would not alter the value of λ_{cr} for which the values of $\bar{B}$ become complex and the motion becomes unstable.

The properties of the equivalent isotropic plate are as follows:

$$\left.\begin{aligned} l_{EFF} &= l \\ w_{EFF} &= w\sqrt{\frac{D_x}{D_{xy}}} \\ D_{EFF} &= D_x \\ t_{EFF} &= \left[12(1 - \nu^2)\frac{D_x}{E}\right]^{1/3} \end{aligned}\right\} \tag{10}$$

where D_{EFF} is the plate stiffness of the equivalent plate, t_{EFF} is the thickness, l_{EFF} is the length, w_{EFF} is the width, ν is Poisson's ratio, and E is Young's modulus of elasticity.

For the corrugation-stiffened panels discussed in this paper, the stiffness properties were obtained as follows: The plate stiffness D_x was calculated for a unit element of the panel shown in the following sketch:

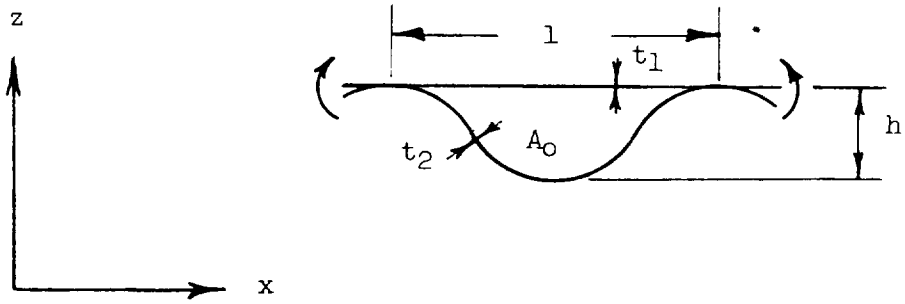

Sketch 2

The element consisted of one corrugation and the cover sheet. The stiffness D_x was obtained by analyzing the element as a structural bent. (See, for example, ref. 5.) The stiffness D_{xy} was obtained from the torsional stiffness of the element shown in sketch 2 by means of the relation

$$\frac{D_{xy}}{G} = \frac{4A_o^2}{\oint \frac{ds}{t}} \tag{11}$$

where A_o is the enclosed area of the torque cell, ds is the length of a differential element of the sheet, t is the sheet thickness, and h is the normalized depth of the corrugation. The properties of the equivalent isotropic plate were obtained from equations (10).

REFERENCES

1. Tuovila, W. J., and Hess, Robert W.: Experimental Investigation of Flutter of Buckled Curved Panels Having Longitudinal Stringers at Transonic and Supersonic Speeds. NASA MEMO 5-18-59L, 1959.

2. Sylvester, Maurice A.: Experimental Studies of Flutter of Buckled Rectangular Panels at Mach Numbers From 1.2 to 3.0 Including Effects of Pressure Differential and of Panel Width-Length Ratio. NACA RM L55I30, 1955.

3. Timoshenko, S.: Theory of Plates and Shells. McGraw-Hill Book Co., Inc., 1940.

4. Hedgepeth, John M.: Flutter of Rectangular Simply Supported Panels at High Supersonic Speeds. Jour. Aero. Sci., vol. 24, no. 8, Aug. 1957, pp. 563-573, 586.

5. Wang, Chu-Kia: Statically Indeterminate Structures. McGraw-Hill Book Co., Inc., 1953.

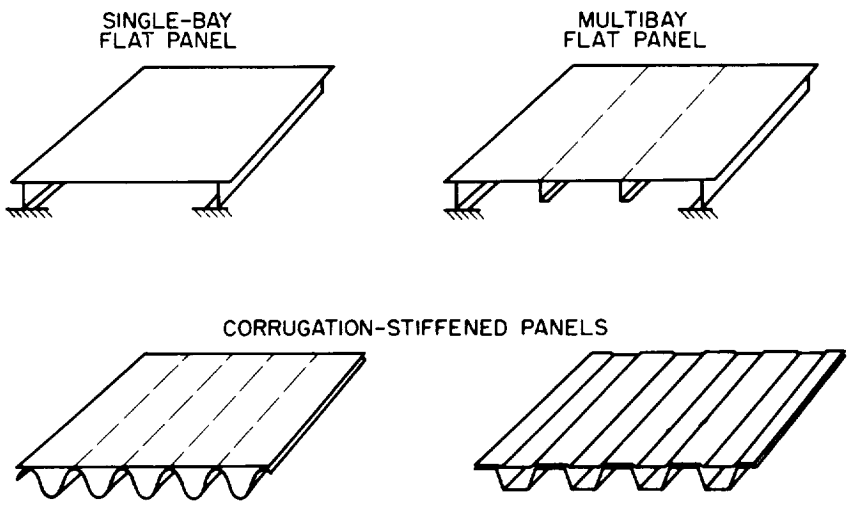

Figure 1

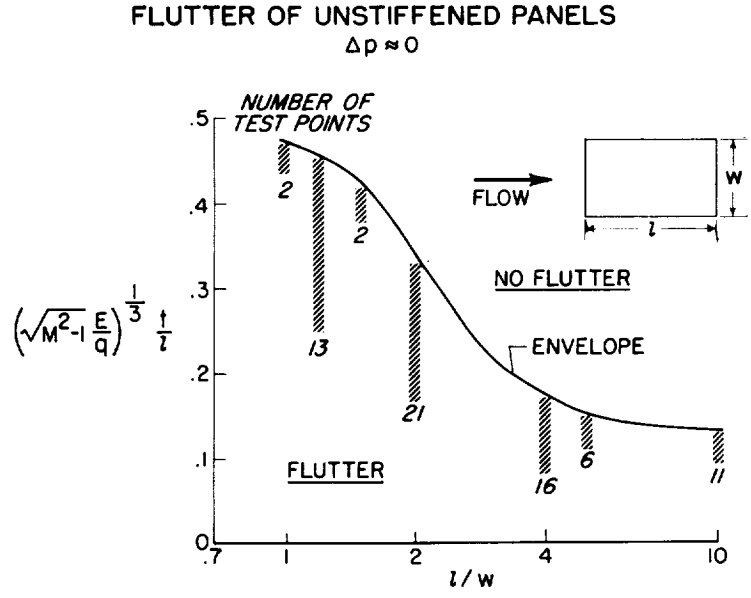

Figure 2

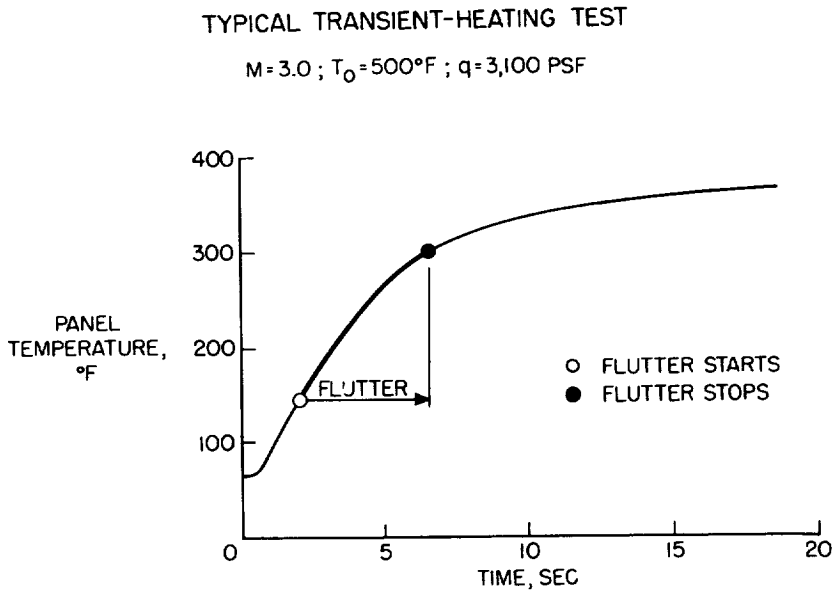

Figure 3

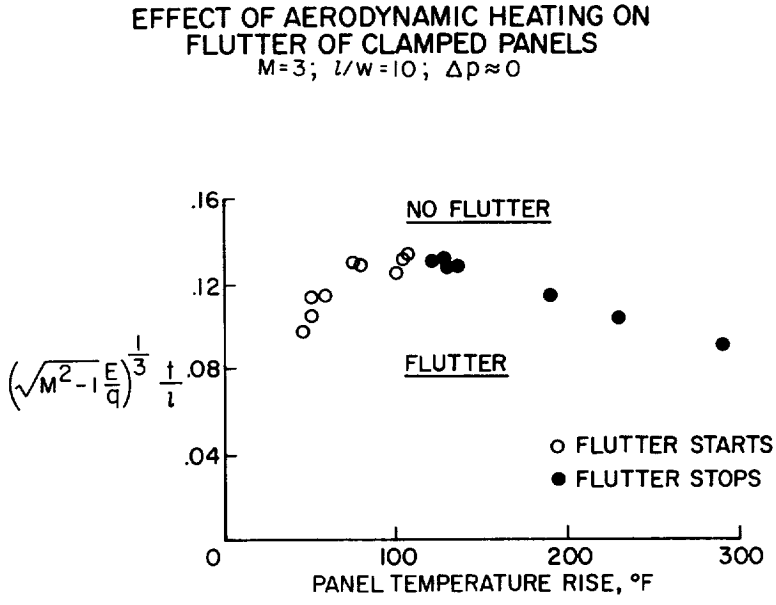

Figure 4

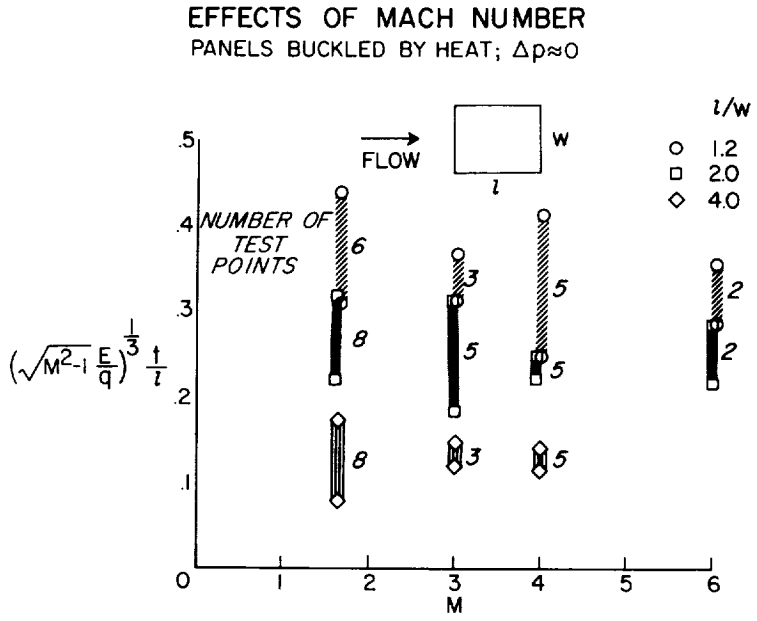

Figure 5

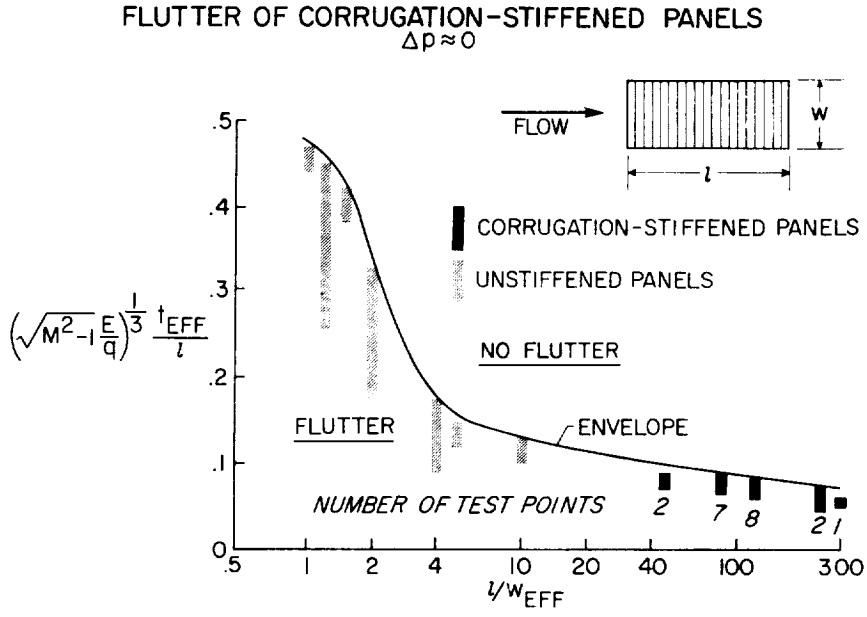

Figure 6

REGIONS OF X-15 RESEARCH AIRCRAFT AFFECTED BY PANEL FLUTTER

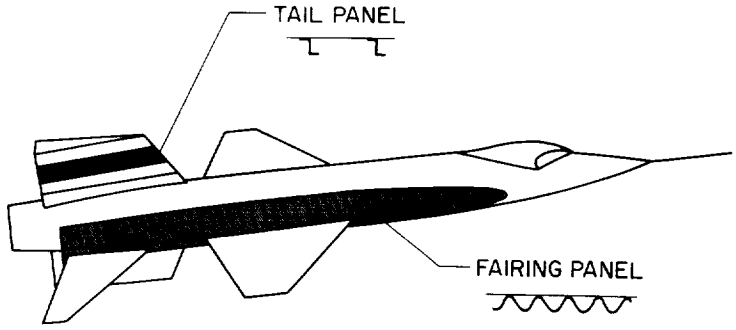

Figure 7

X-15 PANEL-FLUTTER RESULTS

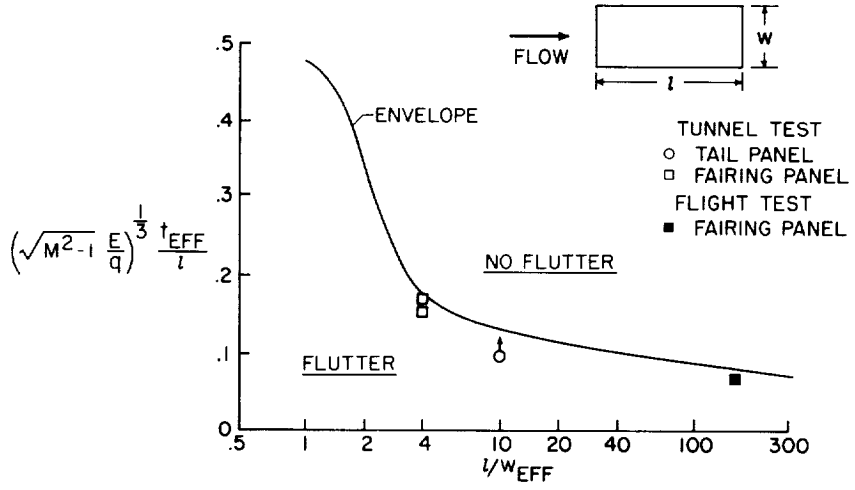

Figure 8

L-1077